3D-printed electrodes

with improved mass transport properties

Jonas Lölsberg[a,b], Ottokar Starck[b], Serafin Stiefel[a,b], Jonas Hereijgers[a,c], Tom Breugelmans[c], Matthias Wessling[a,b,*]

[a] *J. Lölsberg, Dr.-Ing. S. Stiefel, Dr. J. Hereijgers, Prof. Dr.-Ing. M. Wessling, DWI - Leibniz Institute for Interactive Materials, Forckenbeckstr. 50, 52074 Aachen, Germany*

[b] *J. Lölsberg, O. Starck, Dr.-Ing. S. Stiefel, Prof. Dr.-Ing. M. Wessling, RWTH Aachen University, Aachener Verfahrenstechnik-Chemical Process Engineering, Forckenbeckstr. 51, 52074 Aachen, Germany*

[c] *Dr. J. Hereijgers, Prof. Dr. T. Breugelmans, University of Antwerp, Research Group Advanced Reactor Technology, Universiteitsplein 1, 2610 Wilrijk, Belgium*

** Phone: +49-241-8095470, Fax: +49-241-8092252, Manuscripts.cvt@avt.rwth-aachen.de, Forckenbeckstr. 51, 52074 Aachen, Germany*

Abstract

Today's electrochemical reactor design is a less developed discipline as compared to the electrocatalytic synthesis. While catalysts show increasing conversion rates, they are often operated without measures for the reduction of concentration polarization effects. As a result, a stagnant boundary layer forms at the electrode-electrolyte interface. This stagnant boundary layer presents an additional voltage drop and reduces the energy efficiency. It is generally accepted that this phenomenon is caused by a combination of fast electrode reactions and slow diffusion of the reacting species. Our earlier work demonstrated the potential of non-conducting static mixers to reduce concentration polarization effects. However, there are few studies on conductive static mixers applied as electrodes. In this study, we present a new concept of additive manufactured flow through electrode mixers. Our electrode geometry combines a high surface area with mixing properties, diminishing concentration polarization effects of transport-limited reactions. Mass transport properties of these conductive static mixers are evaluated in an additive manufactured electrochemical reactor under controlled conditions by applying the limiting-current method.

Keywords: printed electrodes, additive manufacturing, kinetics, interfaces, concentration polarization

1. Introduction

Commonly, electrochemical research focuses on catalyst materials for new applications. Often standard electrochemical methods are used to quantify the characteristic features of the electrocatalytic reaction with ever growing depth in understanding molecular details.[1-2] Significantly less effort is spent on understanding details of electrodes in real reactor configurations.[3-6] Concentration polarization at the electrode-electrolyte interface is systematically eliminated in ideal electrochemical characterization methods such as the rotating disk electrode, while they are omnipresent in real reactors.[7-13] Fluid control

at electrodes is hence a pre-requisite to obtain electrochemical conversions as characterized and tailored for new electro-catalysts on a microscale.[14-20] Additive manufacturing serves as an example to create new electrodes and electrochemical reactors with functional geometries.[21-25] Below, we present additive manufactured flow through electrode mixers with yet unprecedented geometry and enhanced hydrodynamics. These electrodes serve as an example how to diminish concentration polarization as evidenced by increasing limiting current densities. The electrode geometry is based on our earlier published work applied as turbulence promoter in devices for membrane separation processes.[26] The geometry has been proven to influence concentration polarization effects while operated with complex fluids during filtration.[27] Here we prove that such geometries when made electrically conductive can act as electrodes with improved mass transport properties. In our manuscript we use the term electrode mixer rather than the frequently used term turbulence promoter to avoid technical misconception.

2. Materials and methods

Printing electrodes

The electrode mixer was designed following the details of Fritzmann et al.[26] According to our specifications the electrode of helical architecture was fabricated at the Fraunhofer Institute for Laser Technology ILT applying selective laser melting of stainless steel (X2CrNiMo 17-12-2).[28-30] As shown in Figure 1 and 3(c) the structure is composed of repeating unit cells with two oppositely twisted filaments which have a single point of contact. The center of the upper filament is positioned on the outer diameter of the lower filament. This allows defining the entire geometry by two dimensionless parameters L_m/D_m and d_m/D_m as well as the number of twisted filaments n_m.[26-27] Geometrical characteristics of the additive manufactured electrode as well as the reactor housing are reported in Table 1.

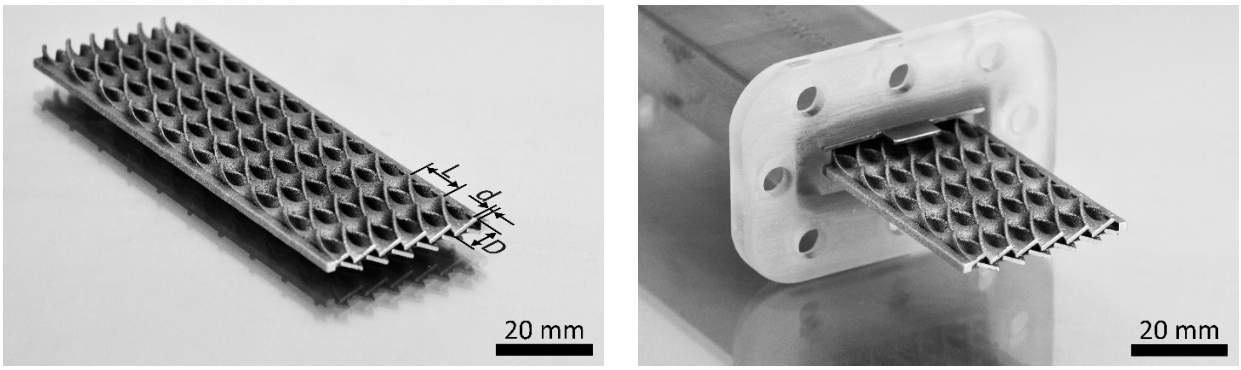

(a) (b)

Figure 1. (a) Electrode mixer of helical architecture, (b) cross-section of the reactor housing including the electrode mixer and the upper flat electrode.

Reactor design

To evaluate mass transport properties for different electrode configurations, an electrochemical reactor housing was designed and fabricated using polyjet 3D printing (Stratasys, Objet Eden 260V).[31] The reactor housing shown in Figure 1(b) and Figure 2 was printed layer by layer with a transparent photopolymer (Stratasys, RGD810). During printing the internal fluid channels need supporting structures (Stratasys,

SUP705) which were later cleaned using a high-pressure washer (Krumm-tec, RK Top 5). Any remaining support was subsequently removed in a stirred bath of 1 mol/L sodium hydroxide for approximately 12 hours.

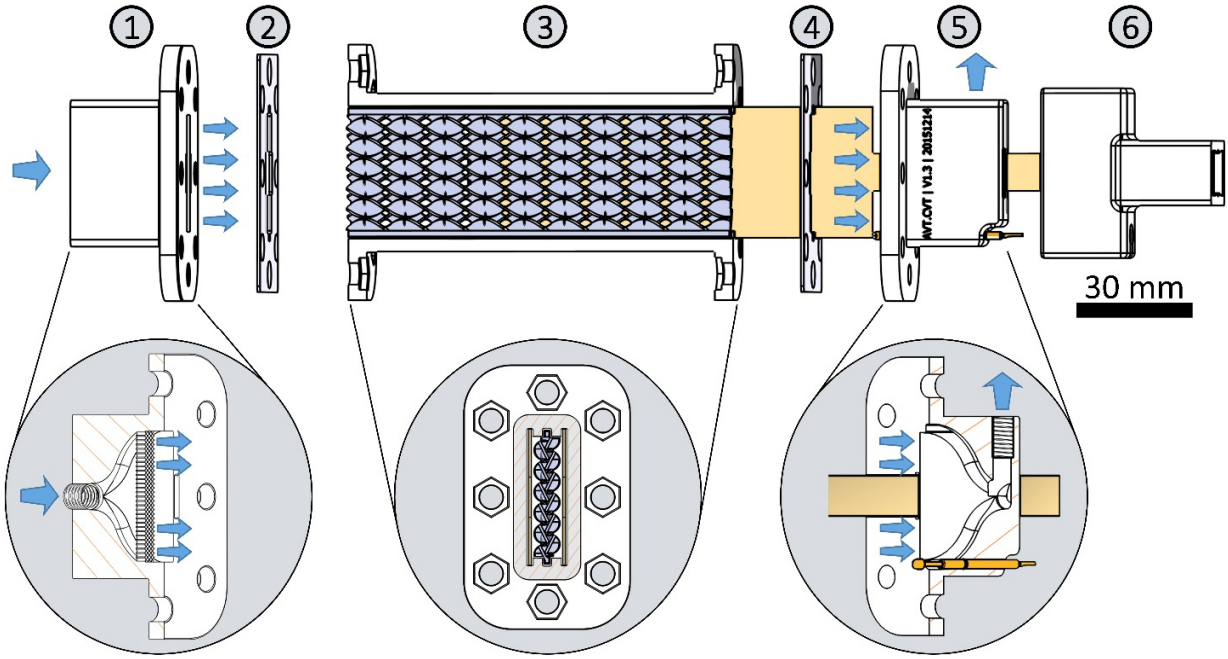

Figure 2. Scheme of the electrochemical reactor consisting of the following parts: (1) flow inlet, (2 & 4) profile gaskets, (3) reactor housing with build-in electrode mixer and two flat electrodes, (5) flow outlet, (6) electrode connector.

The reactor consists of the following functional parts: (1) inlet with an integrated mesh flow distributor with 200 µm pores which generates a uniform flow profile over the entire channel width, (2 & 4) additive manufactured flexible profile gaskets (Stratasys, FLX950), (3) reactor housing with the electrode mixer guided by a rail to maintain the interelectrode gap and two flat stainless steel electrodes, (5) outlet with an embedded gold spring probe pin (Ingun Prüfmittelbau, GKS-003-0040) to connect the electrode mixer, (6) electrical connector for the flat electrodes.

Table 1. Nominal geometrical characteristics of the electrode mixer and the reactor housing. The electrode mixer surface area was obtained from CAD models.

Filament diameter	D_m	5.2	mm
Filament thickness	d_m	0.8	mm
Number of filaments	n_m	~12	-
Filament length (single twist)	L_m	10.4	mm
Electrode mixer height	h_m	6.8	mm
Electrode mixer surface area	A_m	14195.0	mm²
Electrode mixer void fraction	φ_m	77.9	%
Reactor channel height	h_{ch}	7.6	mm
Reactor channel width	w_{ch}	30.0	mm
Reactor channel length	l_{ch}	100.0	mm
Flat electrode surface area	A_e	3000.0	mm²

Fluid dynamics

To perform the experiments under well defined flow conditions, fluid dynamics simulations with Comsol Multiphysics were carried out during the design process of the electrochemical reactor. In particular the inflow conditions were optimized with an integrated mesh flow distributor as shown in Figure 2. In Figure 3 we demonstrate the three dimensional flow distribution at (a) the inlet without flow distributor and (b) the inlet with flow distributor. The three dimensional flow field inside the electrode mixer is visualized by (d) six layers along the flow path of (c) the repeating unit cell. Here, the velocity magnitude is shown by a color-coded background and arrows denote the flow direction. The two different inlet configurations were simulated with laminar inflow conditions and zero pressure at the outlet. Symmetry and periodic boundary conditions were applied to the simulations to reduce calculation effort.

Characterization of the mass transport

Mass transport properties were evaluated for two different electrode configurations using the limiting-current method.[32] An electrolyte was prepared of 5 mM potassium ferrocyanide and a twentyfold excess of potassium ferricyanide in deionised water. Additionally 1 mol/L potassium hydroxide was added as supporting electrolyte. This composition ensures that only the anode reaction regenerates potassium ferricyanide.[4] All prepared chemicals were of analytical grade and used without further purification. The aqueous electrolyte was circulated from a stirred reservoir (Heidolph, MR Hei-Standard) to the reactor compartment via a gear pump (Ismatec, MCP-Z Process IP65) at a constant non-fluctuant flow rate of 40 mL/min. The discharged electrolyte was recycled to the stirred reservoir. Prior to the measurement the electrodes were cleaned, mounted in the reactor housing and connected to a potentiostat (Metrohm, Autolab PGSTAT302N). Once a potential was applied the reversible redox-reaction of potassium ferrocyanide and potassium ferricyanide started to evolve in the reactor compartment.

$$[Fe(CN)_6]^{-4} \rightleftarrows [Fe(CN)_6]^{-3} + e^-$$

Current-potential curves were recorded with chronoamperometry by stepwise increasing the potential from +0.0 V to a maximum of +1.2 V while plotting the current over time. With each change in potential a new steady state was allowed to develop. Steady state current-potential data were obtained after a maximum of 240 seconds. As recorded by the potentiostat we report space averaged data normalized for the effective electrode area. These data were also replotted as the reciprocal resistance against the reciprocal current density. The reciprocal resistance and the reciprocal current density were calculated of the applied potential, the measured current in steady state and the anode surface area. Here, diffusion resistance related to the arising boundary layer can be identified.[33-34] Typically s-shaped curves are observed with under-limiting and over-limiting regions. The point of inflection is designated to the limiting current density I_{lim}/A_{eff}. According to the limiting-current condition a maximum concentration gradient is obtained and potassium ferrocyanide is locally depleted at the anode surface. In steady state, the concentration of potassium ferrocyanide at the anode surface $C_{i,0}$ is considered virtually zero. Since the anolyte and the catholyte are not separated, a depletion of potassium ferrocyanide in the bulk is fully compensated by the cathodic reaction. Hence, the bulk concentration $C_{i,bulk}$ can be considered constant. With these assumptions the mass transfer coefficient k_L can be estimated according to Equation 1.[33-34]

$$k_L = \frac{I_{lim}}{n_e \cdot F \cdot A_{eff} \cdot C_{i,bulk}} \quad (1)$$

Here n_e equals the number of transferred electrons, F is known as the Faraday constant, A_{eff} accounts for the effective anode surface area and $C_{i,bulk}$ is the concentration of the component potassium ferrocyanide in the bulk.[35] The effective anode surface area A_{eff} was determined of the designed models and is shown in Table 1.

3. Results and discussions

To perform the experiments under well defined flow conditions, fluid dynamics simulations were carried out during the design process of the additive manufactured electrochemical reactor. At the inlet, flow conditions were optimized towards a homogeneous distribution by embedding a mesh as visualized in Figure 2, 3(a) and 3(b). Hence, the formation of dead zones and channeling effects inside the reactor housing and at the electrode mixer were prevented.

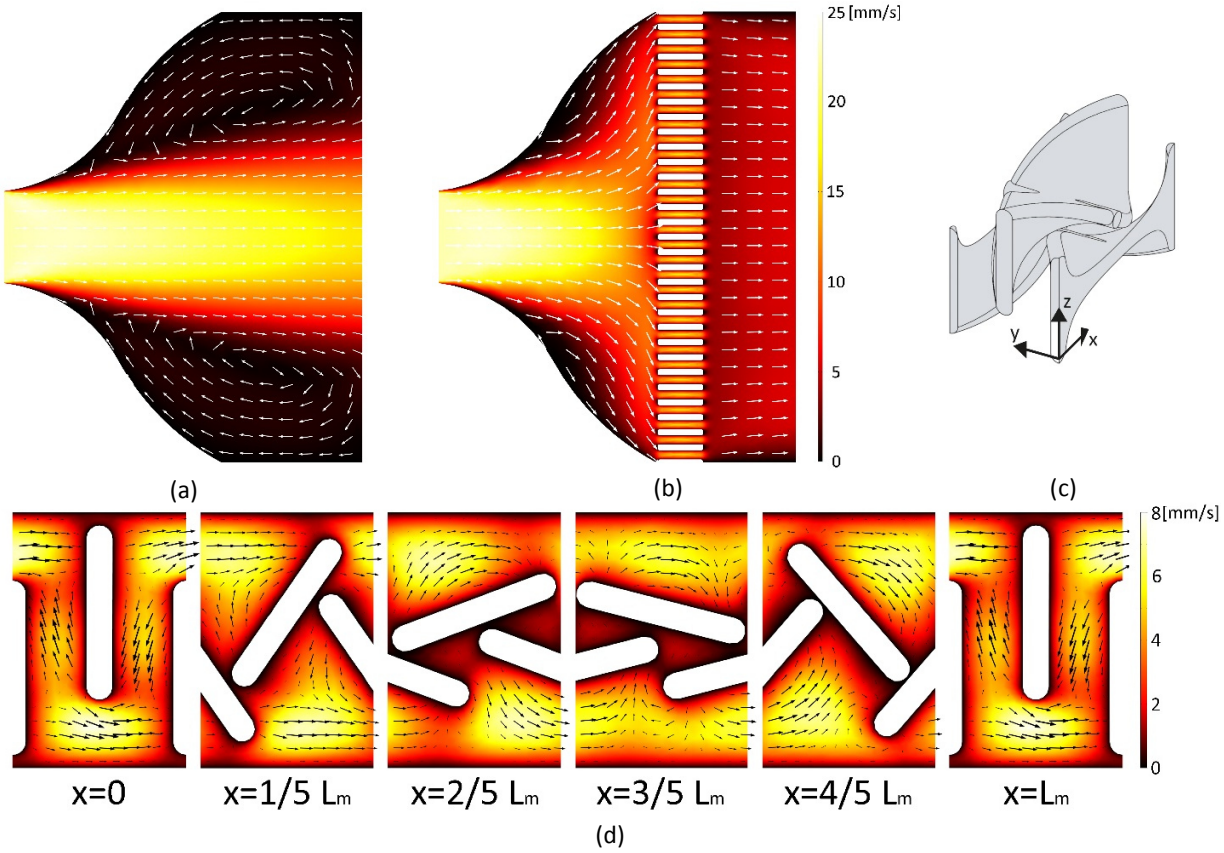

Figure 3. Simulations of the 3D flow field inside (a) the inlet without flow distributor, (b) the inlet with flow distributor and the electrode mixer visualized by (d) six layers along the flow path of (c) the repeating unit cell. The velocity magnitude is shown by a color-coded background and arrows denote the flow direction.

In this article, the effect of the inflow conditions on the electrochemical conversion were not studied. However, former studies showed the positive effect of homogeneous flow conditions on the current

density.[36] The flow field inside the electrode mixer is visualized in Figure 3(d) by six layers along the flow path of the repeating unit cell shown in Figure 3(c). The helical electrode mixer leads to a rotational flow profile reducing the concentration polarization layer at the electrode-electrolyte interface.

The designed electrochemical reactor shown in Figure 2 was operated as an empty channel with two flat electrodes as cathode and anode. By adding the electrode mixer to the reference system the second configuration was set up. Here the electrode mixer was connected as anode and the two flat electrodes were operated as cathodes. The measured raw data are summarized in Figure 4(a). For both electrode configurations the measurements show a similar trend: With increasing applied potentials a limitation of diffusion develops as observed by changes in current curvature. These changes are more pronounced for the configuration without mixer as observed by the formation of a distinct plateau. The formation of a plateau indicates that the entire electrode operates under mass transfer limitation resulting in an evenly formed boundary layer across the entire electrode-electrolyte interface. In contrast a non-uniform laminar boundary layer forms at the surface of the electrode mixer as indicated by a less distinctive plateau. In this case the electrode mixer is disrupting the laminar boundary layer at the electrode-electrolyte interface shifting mass transfer limitation towards a higher potential.

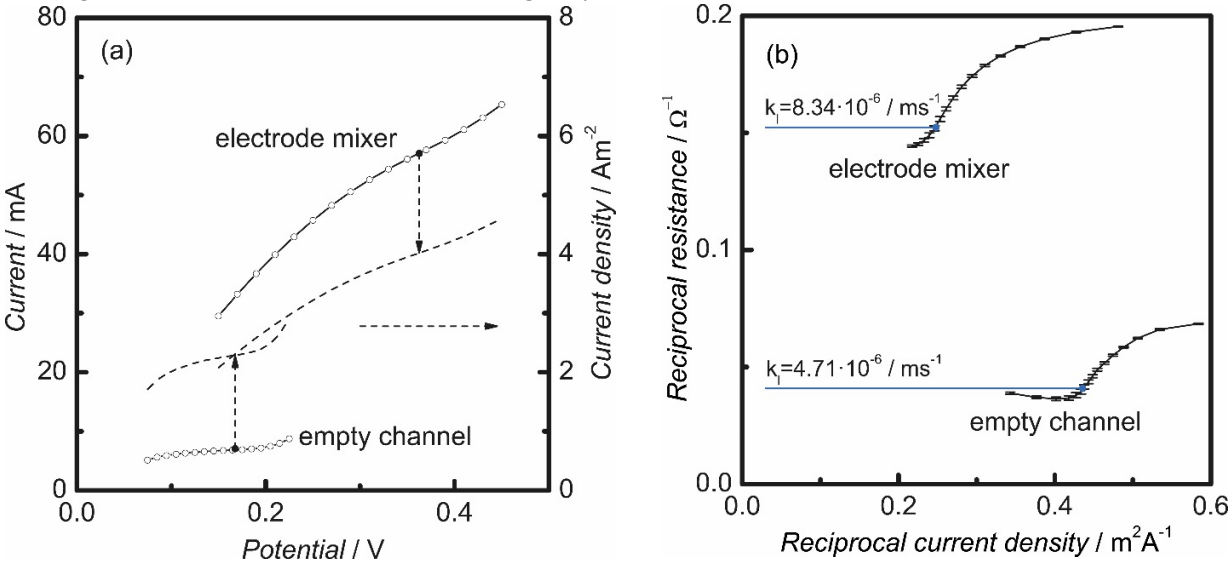

Figure 4. Evaluation of mass transport properties for the reactor configured as empty channel and with electrode mixer. (a) measured raw data, (b) resistance plot. All measurements were repeated three times in a random order. Error bars indicate the measured uncertainty of the reciprocal resistance.

To quantify both electrode configurations in terms of mass transport properties, the current is first normalized by the electrode surface area as indicated by dashed lines in Figure 4(a). When data are visualized in Figure 4(b) as a plot of the reciprocal resistance against the reciprocal current density, mass transport limitations and the formation of a concentration polarization boundary layer appear as rapid changes in resistance.[33] The inflection points representing the limiting current densities are located at 2.28 A/m² (0.17 V) and 4.02 A/m² (0.36 V) for the measurements without and with electrode mixer, respectively. Comparing the mass transport properties reveals an increase of 76 % in mass transport coefficient as the electrode mixer is applied. The increasing mass transport properties are caused by hydrodynamic effects imposed by the electrode mixer: Increased shear forces at the electrode-electrolyte interface lower the thickness of the laminar boundary layer and thereby shorten the distance of

diffusion.[37-38] Our measurements show the feasibility to make use of additive fabrication methods to generate new electrode geometries. The approach, in conjunction with systematic CFD multiphysics modeling, presents a relatively easy way to quickly test and optimize various electrode geometries to suit different electrochemical reactions. Whether the presented electrode geometry also helps to improve the physico-chemical hydrodynamics in gas evolution reactions remains to be investigated in the future. We are confident that the presented evidence stimulates the field of electrochemistry beyond the search of electrocatalysts only.

4. Conclusion

The article describes new electrode architectures printed of stainless steel by an additive manufacturing technique. The geometry has improved mass transport properties as revealed by increased limiting current densities. This work opens a plethora of questions as indicated in the discussion part. In particular, it motivates further research on new electrode geometries in relation to electrochemical phenomena such as gas bubble evolution and polarization in complex 3D architectures.

Acknowledgements

This project has received funding from the European Research Council (ERC) under the European Union's Horizon 2020 research and innovation program (grant agreement No 694946). It was supported by the Alexander-von-Humboldt Foundation and the Cluster of Excellence "Tailor-made Fuels from Biomass" (TMFB) funded by the Excellence Initiative of the German federal and state governments. J. Hereijgers greatly acknowledges the Research Foundation – Flanders (FWO) for support through a Post-Doctoral grant (28761).

References

[1] A. J. Bard, L. R. Faulkner, *Electrochemical methods: fundamentals and applications*, 2 ed., Wiley, **2001.**
[2] J. Newman, K. E. Thomas-Alyea, *Electrochemical systems*, 3 ed., Wiley, **2012**.
[3] J. M. Marracino, F. Coeuret, S. Langlois, *Electrochim. Acta* **1987**, *32*, 1303-1309.
[4] C. J. Brown, D. Pletcher, F. C. Walsh, J. K. Hammond, D. Robinson, *J. Appl. Electrochem.* **1994**, *24*, 95-106.
[5] S. Stiefel, J. Lölsberg, L. Kipshagen, R. Möller-Gulland, M. Wessling, *Electrochem. Commun.* **2015**, *61*, 49-52.
[6] C. J. Brown, D. Pletcher, F. C. Walsh, J. K. Hammond, D. Robinson, *J. Appl. Electrochem.* **1992**, *22*, 613-619.
[7] W. J. Albery, M. L. Hitchman, *Ring-disc electrodes, Vol. 1*, Clarendon Press Oxford, **1971**.
[8] M. Eisenberg, C. W. Tobias, C. R. Wilke, *J. Electrochem. Soc.* **1954**, *101*, 306-320.
[9] A. C. Riddiford, *Adv. Electrochem. El. Eng.* **1966**, *4*, 47-116.
[10] D. E. Fowler, J. M. Haag, C. Boland, D. M. Bierschenk, S. A. Barnett, K. R. Poeppelmeier, *Chem. Mater.* **2014**, *26*, 3113-3120.
[11] D. P. Gregory, A. C. Riddiford, *J. Chem. Soc.* **1956**, 3756-3764.
[12] M. Kundys, W. Adamiak, M. Jönsson-Niedziółka, *Electrochem. Commun.* **2016**, *72*, 46-49.
[13] W. H. Smyrl, J. Newman, *J. Electrochem. Soc.* **1971**, *118*, 1079-1081.
[14] P. Feron, G. S. Solt, *Desalination* **1991**, *84*, 137-152.

[15] I. H. Kim, H. N. Chang, others, *Int. J. Heat Mass Transfer* **1983**, *26*, 1007-1016.
[16] F. B. Leitz, L. Marinčić, *J. Appl. Electrochem.* **1977**, *7*, 473-484.
[17] F. Schwager, P. M. Robertson, N. Ibl, *Electrochim. Acta* **1980**, *25*, 1655-1665.
[18] M. Stern, A. L. Geary, *J. Electrochem. Soc.* **1957**, *104*, 56-63.
[19] A. Storck, F. Coeuret, *Electrochim. Acta* **1977**, *22*, 1155-1160.
[20] A. Storck, D. Hutin, *Electrochim. Acta* **1981**, *26*, 127-137.
[21] A. Ambrosi, J. G. S. Moo, M. Pumera, *Adv. Funct. Mater.* **2016**, *26*, 698-703.
[22] L. F. Arenas, C. P. de León, F. C. Walsh, *Electrochem. Commun.* **2017**, *77*, 133-137.
[23] J. Linkhorst, K. Percin, S. Kriescher, M. Wessling, *Chem. Electro. Chem.* **2017**.
[24] M. D. Symes, P. J. Kitson, J. Yan, C. J. Richmond, G. J. T. Cooper, R. W. Bowman, T. Vilbrandt, L. Cronin, *Nature Chemistry* **2012**, *4*, 349-354.
[25] J. Weber, A. J. Wain, H. Piili, V.-P. Matilainen, A. Vuorema, G. A. Attard, F. Marken, *ChemElectroChem* **2016**, *3*, 1020-1025.
[26] C. Fritzmann, M. Hausmann, M. Wiese, M. Wessling, T. Melin, *J. Membr. Sci.* **2013**, *446*, 189-200.
[27] C. Fritzmann, M. Wiese, T. Melin, M. Wessling, *J. Membr. Sci.* **2014**, *463*, 41-48.
[28] J. P. Kruth, L. Froyen, J. V. Vaerenbergh, P. Mercelis, M. Rombouts, B. Lauwers, *J. Mater. Process. Technol.* **2004**, *149*, 616-622.
[29] W. Meiners, *Direktes selektives Laser Sintern einkomponentiger metallischer Werkstoffe*, 1 ed., **Shaker**, 1999.
[30] R. Poprawe, *Lasertechnik für die Fertigung*, 1 ed., **Springer**, 2005.
[31] I. Gibson, D. W. Rosen, B. Stucker, others, *Additive manufacturing technologies, Vol. 238*, Springer, **2010**.
[32] L. P. Reiss, T. J. Hanratty, *AlChE J.* **1962**, *8*, 245-247.
[33] D. A. Cowan, J. H. Brown, *Ind. Eng. Chem.* **1959**, *51*, 1445-1448.
[34] J. R. Selman, C. W. Tobias, *Adv. Chem. Eng.* **1978**, *10*, 211-318.
[35] F. Li, W. Meindersma, A. B. de Haan, T. Reith, *J. Membr. Sci.* **2004**, *232*, 19-30.
[36] A. P. Manso, F. F. Marzo, J. Barranco, X. Garikano, M. G. Mujika, *Int. J. Hydrogen Energy* **2012**, *37*, 15256-15287.
[37] B. Levich, *Discuss. Faraday Soc.* **1947**, *1*, 37-49.
[38] H. Schlichting, K. Gersten, *Boundary-layer theory*, Springer Science & Business Media, **2003**.

Table of Contents

A new concept of additive manufactured flow through electrode mixers is presented. The electrode geometry combines a high surface area with mixing properties, diminishing concentration polarization effects of transport-limited reactions.